

# HYDROGENATION OF CARBON DIOXIDE OVER A SUPPORTED RUTHENIUM CATALYST

by

Frank L. Kester\*

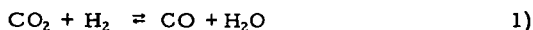
Hamilton Standard  
Division of United Aircraft Corporation  
Windsor Locks, Connecticut 06096

## INTRODUCTION

The ever increasing demand for natural gas as a fuel and raw material has stimulated renewed efforts to find other ways of producing methane. With more and more evidence of an "energy crisis" upon us, alternative approaches such as catalytically synthesizing methane from hydrogen and carbon dioxide meet with more promise of development.

A fairly complete summary of the research on carbon dioxide methanation has been given by Emmett (5), and details of the carbon monoxide-hydrogen reactions by Kirk and Othmer (10). Recent studies on the reaction between hydrogen and carbon dioxide over a supported nickel catalyst have been conducted by Binder and White (1) and by Dew *et al.* (3). Hydrogenation of carbon monoxide over a nickel catalyst has also been investigated (6). A few years ago, Karn and his associates (9) studied ruthenium as a possible methanation catalyst. In a recent experiment, Lunde and Kester (13) studied the reaction rates of methane production from hydrogen and carbon dioxide. The work described here is an extension of this effort, and presents the kinetics and possible mechanisms for the reaction between hydrogen and carbon dioxide.

It is believed by many workers (5) that carbon monoxide is a critical intermediate in carbon dioxide methanation. The following reactions summarize the overall reduction process.



Because the equilibrium for Equation 1 is somewhat unfavorable at the reaction temperatures (200°-400° C), it can be argued that this reaction path is somewhat unlikely. A way out of this difficulty is to require that at these temperatures the methanation of carbon monoxide (Reaction 2) proceeds much faster than carbon monoxide production (Reaction 1). Reaction 2 could be in equilibrium. If carbon monoxide were rapidly consumed as it formed, no carbon monoxide would be observed in the reactor exit stream. This was the case with the data treated here (13). However, in his work with a ruthenium catalyst, Karn (9) did observe 1.5-2% carbon monoxide in the exit stream. The reason for his observation

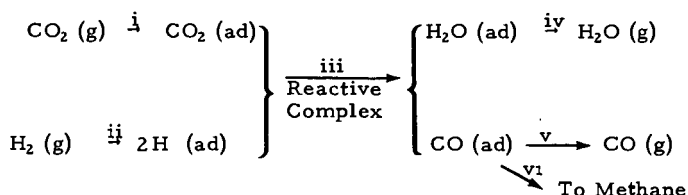
\* Present address: Institute of Gas Technology, 3424 S. State Street, Chicago, Illinois 60616

is not clear. It is possible that because of the extended operation (80 days) the catalyst may have become deactivated for the reaction converting carbon monoxide to methane.

## REACTION MECHANISMS

### Mechanism I

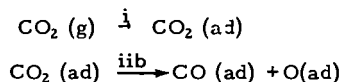
The reaction mechanism outlined here follows the work of Oki and Mezaki (14, 15) for the water-gas-shift reaction over iron oxide.



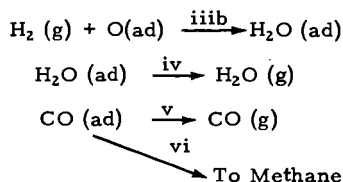
The absorbed carbon monoxide is ultimately reduced to methane by some reaction path not examined here. For the rate model developed in the next section, the reaction of  $2\text{H}(\text{ad})$  and  $\text{CO}(\text{ad})$  (step iii) is assumed to offer the controlling resistance. The other reactions are assumed to be in equilibrium.

### Mechanism II

An alternative mechanism, first suggested by Doehlemann (4) in 1938 and subsequently by Kul'kova and his coworkers (11, 12), has been described by Wagner (17). The catalyst was also iron oxide; however, the reaction temperatures were much higher ( $870^\circ\text{--}1122^\circ\text{C}$ ) than in Oki and Mezaki's work ( $400^\circ\text{--}450^\circ\text{C}$ ) and higher than in these data ( $207^\circ\text{--}371^\circ\text{C}$ ) on ruthenium. This mechanism is included because it displays the observed dependence on both hydrogen and carbon dioxide, each to the first power (Table 2); it does not contain the hydrogen adsorption constant in its expression (which was found to be very small or zero); and it does not require the presence of three active sites indicated in Mechanism I (which may be somewhat improbable). The alternative mechanism (17) is -



Adsorbed oxygen atoms react with molecular hydrogen in a single step:



This mechanism assumes that step iiib is rate-controlling and that the other steps are in equilibrium. \*

#### RATE EQUATIONS

The model follows Hougen and Watson (7, 8) and employs a Langmuir-Hinshelwood rate model for Mechanism I. The modifications necessary for Mechanism II are given in the footnote below.

Assuming reaction step iii, Mechanism I, as rate-controlling, and with i, ii, iv, v, and vi in equilibrium, the following rate expression can be written:

$$r = k_F \theta_H^2 \theta_{CO_2} \quad 3)$$

where  $r$  is the forward reaction rate,  $k_F$  is the forward reaction rate coefficient, and  $\theta_i$  represents the fraction of catalyst surface coverage of the  $i$ th species.

The surface concentrations in equilibrium with the gaseous reactants or products can be represented by -

$$\theta_H^2 = K_{H_2} P_{H_2} \theta_V^2 \quad 4)$$

$$\theta_{CO_2} = K_{CO_2} P_{CO_2} \theta_V \quad 5)$$

$$\theta_{H_2O} = K_{H_2O} P_{H_2O} \theta_V \quad 6)$$

$$\theta_{CO} = K_{CO} P_{CO} \theta_V \quad 7)$$

where  $\theta_V$  is the fraction of vacant catalyst surface,  $P_i$  is the equilibrium partial pressure, and  $K_i$  is the equilibrium absorption constant of the  $i$ th species.

Inserting relationships 4 and 5 into Equation 3 gives -

$$r = k \theta_V^3 P_{H_2} P_{CO_2} \quad 8)$$

where

$$k = k_F K_{H_2} K_{CO_2} \quad 9)$$

The total fraction surface coverage is equal to the sum of all occupied and unoccupied sites, which equals unity -

---

\* Mechanism II would modify the rate expression by reducing the exponent in the denominator of Equation 14 (presented later) to one and also eliminate  $P_{H_2}^{1/2} K_{H_2}^{1/2}$  from the denominator of this expression.

$$1 = \theta_V + \theta_H + \theta_{CO_2} + \theta_{CO} + \theta_{H_2O} \quad 10)$$

On inserting Equations 4, 5, 6, and 7 into Equation 10, one obtains -

$$1 = \theta_V + P_{H_2}^{1/2} K_{H_2}^{1/2} \theta_V + P_{CO_2} K_{CO_2} \theta_V + P_{CO} K_{CO} \theta_V + P_{H_2O} K_{H_2O} \theta_V \quad 11)$$

which, on solving for  $\theta_V^3$ , yields -

$$\theta_V^3 = 1/[1 + P_{H_2}^{1/2} K_{H_2}^{1/2} + P_{CO_2} K_{CO_2} + P_{CO} K_{CO} + P_{H_2O} K_{H_2O}]^3 \quad 12)$$

Given the Arrhenius relationship

$$k = Ae^{-Ea/RT} \quad 13)$$

and upon inserting Equations 12 and 13 into Equation 8, the final relationship obtained for correlation with the experimental data is -

$$r = Ae^{-Ea/RT} \frac{P_{H_2} P_{CO_2}}{[1 + P_{H_2}^{1/2} K_{H_2}^{1/2} + P_{CO_2} K_{CO_2} + P_{CO} K_{CO} + P_{H_2O} K_{H_2O}]^3} \quad 14)$$

where\*

$$r = \text{reaction rate} = - \frac{dP_{CO_2}}{dt}$$

A = pre-exponential factor

Ea = activation energy, cal/mole

R = 1.987 cal/deg-mole

T = degrees Kelvin

To evaluate this equation and to determine unknown constants, Equation 14 was rearranged as follows -

$$Y \equiv \ln \frac{r}{P_{H_2} P_{CO_2}} = \ln \frac{[1 + K_{H_2}^{1/2} P_{H_2}^{1/2} + K_{CO_2} P_{CO_2} + K_{CO} P_{CO} + K_{H_2O} P_{H_2O}]^3}{P_{H_2} P_{CO_2}} \quad 15)$$

\* Other constants are the same as defined earlier.

where -

$$Y \equiv \ln A - \frac{E_a}{R} \left( \frac{1}{T} \right) \quad (16)$$

After  $Y$  has been evaluated, the rate expression is then of the form  $Y = mX + b$ , so that a plot of  $Y$  versus  $1/T$  for several runs forms a line with a slope  $-E_a/R$  and a  $1/T = 0$  intercept of  $\ln k$ . If the correlation is good, the plot will show minimum scatter and good linearity when a proper form the rate equation has been chosen or a proper value of an adsorption coefficient has been obtained. A least squares calculation of a number of data points will give  $\sigma$ , the standard deviation.

The 62 data points shown in Table 1 contained experimental information on space velocity, average methane partial pressure ( $P_{CH_4}$ ), average water vapor partial pressure ( $P_{H_2O}$ ), and reactor temperature  $^{\circ}(T)$ . The equilibrium carbon monoxide partial pressure,  $P_{CO}$ , was obtained from -

$$P_{CO} = \frac{P_{CH_4} P_{H_2O}}{P_{H_2}^3 K_2} \quad (17)$$

using average experimental partial pressures and  $K_2$ , the equilibrium constant for Reaction 2. The value  $K_2$  was calculated as equal to  $\exp(1/1.987)(0.00266T + 23095.T^{-1} - 17688.T^{-2} + 17.600 - 6.744\ln T)$  from data contained in Reference 16.

The experimental reaction rate,  $r$ , was calculated as -

$$r = S_v (P_{CO_{2in}} - P_{CO_{2out}}) \quad (18)$$

where -

$S_v$  is the experimental space velocity,

$P_{CO_{2in}}$  is the partial pressure of  $CO_2$  at the reactor inlet, and

$P_{CO_{2out}}$  is the partial pressure of  $CO_2$  at the reactor outlet.

## DISCUSSION

### Determination of Form of Rate Equations

The minimum least squares standard deviation,  $\sigma$ , was taken as a quantitative measure of a fit of the data when correlating various forms of the driving force portion of the rate equation. Adsorption coefficients are treated below. The rate data treated are summarized in Table 1.

Table 1. SUMMARY OF EXPERIMENTAL TEST POINTS  
(Data from Reference 13)

TEST NUMBER	REACTOR (DEG. F.)	REACTOR (DEG. C.)	PC02 CONCENTRATION (ATM/HR)	SPACE VELOCITY (11/HR)	INLET TEMP. (DEG. F.)	INLET TEMP. (DEG. C.)	OUTLET TEMP. (DEG. F.)	OUTLET TEMP. (DEG. C.)	INLET TEMP. (DEG. F.)	INLET TEMP. (DEG. C.)	OUTLET TEMP. (DEG. F.)	OUTLET TEMP. (DEG. C.)	INLET TEMP. (DEG. F.)	INLET TEMP. (DEG. C.)	OUTLET TEMP. (DEG. F.)	OUTLET TEMP. (DEG. C.)
519.00	404	207	16.780	2834	0.2117	0.2036	0.2002	0.0033	0.7894	0.0	0.7894	0.0	0.7894	0.0	0.7894	0.0
520.00	433	223	32.730	3005	0.2117	0.1978	0.1911	0.3091	0.7828	0.0	0.7828	0.0	0.7828	0.0	0.7828	0.0
520.10	433	223	25.810	5945	0.4172	0.2047	0.2015	0.4052	0.7893	0.0	0.7893	0.0	0.7893	0.0	0.7893	0.0
521.00	443	228	38.310	5649	0.4172	0.2047	0.2015	0.4052	0.7893	0.0	0.7893	0.0	0.7893	0.0	0.7893	0.0
521.10	443	228	38.310	5649	0.4172	0.2047	0.2015	0.4052	0.7893	0.0	0.7893	0.0	0.7893	0.0	0.7893	0.0
522.10	505	263	141.000	6337	0.4243	0.2055	0.1899	0.3050	0.7422	0.0	0.7422	0.0	0.7422	0.0	0.7422	0.0
523.10	500	260	105.500	5828	0.4256	0.1714	0.1575	0.6814	0.6257	0.1000	0.6257	0.1000	0.6257	0.1000	0.6257	0.1000
524.00	527	275	127.400	5801	0.4231	0.1790	0.1645	0.6818	0.6254	0.0987	0.6254	0.0987	0.6254	0.0987	0.6254	0.0987
525.00	527	275	127.400	5801	0.4231	0.1790	0.1645	0.6818	0.6254	0.0987	0.6254	0.0987	0.6254	0.0987	0.6254	0.0987
526.00	527	275	127.400	5801	0.4231	0.1790	0.1645	0.6818	0.6254	0.0987	0.6254	0.0987	0.6254	0.0987	0.6254	0.0987
527.00	553	289	115.200	5319	0.4231	0.1487	0.1331	0.3370	0.4721	0.2141	0.4721	0.2141	0.4721	0.2141	0.4721	0.2141
527.10	559	293	123.500	5334	0.4231	0.1485	0.1316	0.2598	0.4409	0.2197	0.4409	0.2197	0.4409	0.2197	0.4409	0.2197
527.20	569	298	142.500	5334	0.4231	0.1485	0.1291	0.3258	0.4490	0.2197	0.4490	0.2197	0.4490	0.2197	0.4490	0.2197
528.00	598	314	178.000	5125	0.4223	0.1243	0.0983	0.3362	0.3280	0.2765	0.3280	0.2765	0.3280	0.2765	0.3280	0.2765
528.10	598	314	178.000	5125	0.4223	0.1243	0.0983	0.3362	0.3280	0.2765	0.3280	0.2765	0.3280	0.2765	0.3280	0.2765
530.00	624	328	222.800	5150	0.4223	0.1225	0.0916	0.4295	0.2878	0.3004	0.2878	0.3004	0.2878	0.3004	0.2878	0.3004
531.00	652	344	252.000	5235	0.4223	0.1229	0.0846	0.4202	0.2598	0.3059	0.2598	0.3059	0.2598	0.3059	0.2598	0.3059
532.00	652	344	64.010	4956	0.4083	0.0714	0.0594	0.1805	0.1298	0.5023	0.1298	0.5023	0.1298	0.5023	0.1298	0.5023
539.50	423	217	26.910	4956	0.4083	0.3415	0.3374	0.6854	0.6467	0.0	0.6467	0.0	0.6467	0.0	0.6467	0.0
540.00	440	227	36.660	5016	0.4083	0.3435	0.3388	0.6633	0.6392	0.0	0.6392	0.0	0.6392	0.0	0.6392	0.0
540.80	450	232	46.630	5062	0.4083	0.3435	0.3388	0.6633	0.6392	0.0	0.6392	0.0	0.6392	0.0	0.6392	0.0
541.10	485	252	86.620	5192	0.4063	0.3455	0.3379	0.6613	0.6117	0.0	0.6117	0.0	0.6117	0.0	0.6117	0.0
541.10	485	252	86.620	5192	0.4063	0.3455	0.3380	0.6613	0.6117	0.0	0.6117	0.0	0.6117	0.0	0.6117	0.0
542.00	500	253	125.300	5176	0.4070	0.3454	0.3336	0.6634	0.5955	0.0	0.5955	0.0	0.5955	0.0	0.5955	0.0
543.00	505	257	155.430	4741	0.4070	0.3305	0.3264	0.5117	0.4762	0.1051	0.4762	0.1051	0.4762	0.1051	0.4762	0.1051
544.00	512	267	96.920	4782	0.4070	0.3312	0.3241	0.5124	0.4507	0.1081	0.4507	0.1081	0.4507	0.1081	0.4507	0.1081
544.10	520	271	103.900	4815	0.4070	0.3317	0.3236	0.5124	0.4406	0.1081	0.4406	0.1081	0.4406	0.1081	0.4406	0.1081
544.20	528	276	151.600	4819	0.4070	0.3317	0.3208	0.5124	0.4170	0.1081	0.4170	0.1081	0.4170	0.1081	0.4170	0.1081
545.00	518	271	85.050	4977	0.4070	0.3302	0.3226	0.4476	0.3872	0.1543	0.3872	0.1543	0.3872	0.1543	0.3872	0.1543
545.10	528	276	93.110	4624	0.4070	0.3302	0.3220	0.4476	0.3882	0.1543	0.3882	0.1543	0.3882	0.1543	0.3882	0.1543
545.30	534	279	107.400	4626	0.4070	0.3302	0.3209	0.4476	0.3722	0.1543	0.3722	0.1543	0.3722	0.1543	0.3722	0.1543
546.10	541	283	121.500	4668	0.4078	0.3276	0.3182	0.4437	0.3593	0.1587	0.3593	0.1587	0.3593	0.1587	0.3593	0.1587
547.00	572	300	154.320	4177	0.4070	0.2647	0.2568	0.1526	0.1091	0.3941	0.1091	0.3941	0.1091	0.3941	0.1091	0.3941
548.00	587	308	64.570	4276	0.4070	0.2647	0.2568	0.1526	0.0914	0.3941	0.0914	0.3941	0.0914	0.3941	0.0914	0.3941
549.10	590	310	133.500	4404	0.4070	0.2865	0.2729	0.2477	0.1379	0.3164	0.1379	0.3164	0.1379	0.3164	0.1379	0.3164
550.00	610	324	167.500	4497	0.4070	0.2855	0.2686	0.2502	0.1146	0.3154	0.1146	0.3154	0.1146	0.3154	0.1146	0.3154
551.00	640	338	176.200	4560	0.4067	0.2817	0.2598	0.6846	0.2220	0.161	0.2220	0.161	0.2220	0.161	0.2220	0.161
560.00	601	321	363.200	4939	0.4087	0.3237	0.2993	0.4848	0.72492	0.1378	0.72492	0.1378	0.72492	0.1378	0.72492	0.1378
562.00	602	317	270.100	4721	0.4059	0.3151	0.2923	0.4142	0.2214	0.1605	0.2214	0.1605	0.2214	0.1605	0.2214	0.1605
563.00	598	313	210.000	4587	0.4059	0.3017	0.2824	0.3468	0.1880	0.2400	0.1880	0.2400	0.1880	0.2400	0.1880	0.2400
564.00	588	309	151.100	4361	0.4059	0.2855	0.2721	0.2362	0.1268	0.3214	0.1268	0.3214	0.1268	0.3214	0.1268	0.3214
565.00	588	309	131.900	4565	0.4321	0.1708	0.1305	0.3950	0.5314	0.1082	0.5314	0.1082	0.5314	0.1082	0.5314	0.1082
566.00	596	314	247.600	5242	0.4321	0.1716	0.1305	0.3950	0.5314	0.1082	0.5314	0.1082	0.5314	0.1082	0.5314	0.1082
567.00	611	325	418.700	5242	0.4321	0.2258	0.1860	0.5672	0.3422	0.1550	0.3422	0.1550	0.3422	0.1550	0.3422	0.1550
568.00	611	325	418.700	5242	0.4321	0.2258	0.1860	0.5672	0.3422	0.1550	0.3422	0.1550	0.3422	0.1550	0.3422	0.1550
570.00	531	277	201.900	5670	0.4311	0.2623	0.2436	0.7514	0.0561	0.0	0.0561	0.0	0.0561	0.0	0.0561	0.0
571.00	527	275	122.000	4971	0.4311	0.2226	0.2078	0.5567	0.4820	0.1567	0.4820	0.1567	0.4820	0.1567	0.4820	0.1567
572.00	528	276	85.100	4552	0.4311	0.1921	0.1807	0.5185	0.3571	0.2492	0.3571	0.2492	0.3571	0.2492	0.3571	0.2492
573.00	524	273	86.150	4231	0.4311	0.1604	0.1323	0.2654	0.2263	0.3895	0.2263	0.3895	0.2263	0.3895	0.2263	0.3895
575.00	524	273	86.150	4231	0.4311	0.1604	0.1323	0.2654	0.2263	0.3895	0.2263	0.3895	0.2263	0.3895	0.2263	0.3895
576.00	527	275	62.320	4387	0.4082	0.2828	0.2755	0.2592	0.2179	0.3063	0.2179	0.3063	0.2179	0.3063	0.2179	0.3063
577.00	528	276	73.800	4581	0.4082	0.3000	0.2823	0.3700	0.3153	0.2288	0.3153	0.2288	0.3153	0.2288	0.3153	0.2288
578.00	529	276	90.360	4754	0.4082	0.3089	0.3003	0.4350	0.3728	0.1806	0.3728	0.1806	0.3728	0.1806	0.3728	0.1806
579.00	530	277	151.000	5332	0.4082	0.3306	0.3195	0.6270	0.5453	0.0386	0.5453	0.0386	0.5453	0.0386	0.5453	0.0386
580.00	530	277	151.000	5332	0.4082	0.3306	0.3195	0.6270	0.5453	0.0386	0.5453	0.0386	0.5453	0.0386	0.5453	0.0386
581.00	531	277	184.600	5644	0.4558	0.3377	0.3253	0.6760	0.5837	0.0	0.5837	0.0	0.5837	0.0	0.5837	0.0

Since some of the data were collected at moderate to high conversions, an initial screening was conducted on all runs to determine if any were close to the thermodynamic limit. Two runs were found to be closer than 5% (Runs 533 and 534 in Ref. 13) of the thermodynamic limit and were not included in the final treatment. This means that any influence by the reverse reaction, Equation 1, on the rate data was no greater than 5% and for most runs was much less than 1%.

If one assumed that the adsorption of hydrogen is rate-controlling (reaction path i), then  $\sigma$  is found to be equal to 0.3305 (Table 2); if the adsorption of carbon dioxide is assumed to be controlling (reaction path ii),  $\sigma$  is 0.4688. It appears that assuming hydrogen to be in equilibrium is consistent with Bond (2), who has summarized the activation energies and pre-exponential factors for hydrogen reactions on various transition metals. Bond indicates an activation energy for hydrogen adsorption generally around 5 kcal and never greater than 10.6 kcal. It appears that a lower activation energy than was observed for these data (18.33 kcal) is necessary for the adsorption of hydrogen onto active metal sites to be controlling. Bond also tabulates pre-exponential factors that would indicate reaction rates much faster than observed for these data.

Secondly, the adsorption of carbon dioxide was not considered to be rate-controlling, as the resulting rate equation would not reflect the preferred dependence on the rate on  $P_{H_2}$  to the first power (Table 2). Oki and Mezaki (14) also considered the possibility of only one adsorbed hydrogen atom reacting with one adsorbed carbon dioxide molecule. This would reflect a dependence of  $P_{H_2}$  to the one-half power with  $P_{CO_2}$  to the first power in the rate equation. This relationship, when correlated with the data, yields an unsatisfactorily high standard deviation of 0.3165.

The most significant improvement and the best correlation of the data with the driving force expression were obtained with a dependence of  $P_{H_2}P_{CO_2}$  (both to the first power) giving a  $\sigma$  of 0.2113. This expression suggests a rate-controlling reaction of two adsorbed hydrogen atoms with one adsorbed carbon dioxide molecule (Mechanism I) or the reaction of gaseous hydrogen with an adsorbed oxygen atom (Mechanism II).

#### Determination of Adsorption Coefficients

With this form of the rate expression, further least squares calculations were performed to evaluate the various adsorption constants. A constant such as  $K_{CO_2}$  would be systematically varied on a trial-and-error basis until a minimum was obtained in the  $\sigma$  versus  $K_{CO_2}$  curve (Figure 1). The other adsorption constants were also evaluated in this manner. The minimum values for the adsorption constants are given in Table 3. Minimum values were obtained for all reaction gases except hydrogen. The  $\sigma$  versus  $K_{H_2}$  curve (not shown) was quite broad and shallow in the region of  $K_{H_2}$  below  $10^{-3}$  atm $^{-1}$ . Apparently these experimental data are not of sufficient quality to obtain a precise value of  $K_{H_2}$ , which is therefore reported to be less than  $10^{-3}$  atm $^{-1}$  for this temperature range. No temperature dependence of the adsorption constants was included in the evaluation.

Table 2. FIT OF RATE EQUATION TO EXPERIMENT DATA

Form of Rate Equation*	Least Squares Standard Deviation, $\sigma$
------------------------	--

## Driving Force Evaluation

$P_{H_2}$	0.3305
$P_{CO_2}$	0.4688
$P_{H_2}^{1/2}$	0.3708
$P_{H_2}^{1/2} P_{CO_2}$	0.3165
$P_{H_2} P_{CO_2}$	0.2113

## Adsorption Coefficient Evaluation

$\frac{P_{H_2} P_{CO_2}}{[1 + K_{CO_2} P_{CO_2}]}$	0.1818
$\frac{P_{H_2} P_{CO_2}}{[1 + K_{CO} P_{CO_2}]^2}$	0.1795
$\frac{P_{H_2} P_{CO_2}}{[1 + K_{CO_2} P_{CO_2}]^3}$	0.1294
$\frac{P_{H_2} P_{CO_2}}{[1 + K_{CO_2} P_{CO_2} + K_{CO} P_{CO}]^3}$	0.1157
$\frac{P_{H_2} P_{CO_2}}{[1 + K_{CO_2} P_{CO_2} + K_{CO} P_{CO} + K_{H_2O} P_{H_2O}]^3}$	0.1144
$\frac{P_{H_2} P_{CO_2}}{[1 + K_{CO_2} P_{CO_2} + K_{CO} P_{CO}]}$	0.1680
$\frac{P_{H_2} P_{CO_2}}{[1 + K_{CO_2} P_{CO_2} + K_{CO} P_{CO} + K_{H_2O} P_{H_2O}]}$	0.1650

\* Driving force and adsorption terms only



Table 3. EVALUATION OF ADSORPTION CONSTANTS FOR 1/2% RUTHENIUM ON ALUMINA\*

<u>Adsorption Constant</u>	<u>Experimental Value, atm<sup>-1</sup></u>
MECHANISM I	
$K_{\text{CO}_2}$	0.760
$K_{\text{H}_2}$	$< 10^{-3}$
$K_{\text{CO}}$	475
$K_{\text{H}_2\text{O}}$	0.160
MECHANISM II	
$K_{\text{CO}_2}$	2.62
$K_{\text{H}_2}$	$< 10^{-3}$
$K_{\text{CO}}$	1490
$K_{\text{H}_2\text{O}}$	0.491

\* Determined by the least squares trial-error fit of the 62 data points over a temperature range of 207°-358°C. These are average constants for this temperature range.

For Mechanism I, the various adsorption constants included in Equation 15, the least squares calculation for the 62 data points, gave a correlation of  $\sigma = 0.999$ . The resulting curve is shown in Figure 2. The activation energy was found to be 18.33 kcal/mole, and the pre-exponential factor was  $3.524 \times 10^{10} \text{ atm}^{-1} \text{ hr}^{-1}$ .

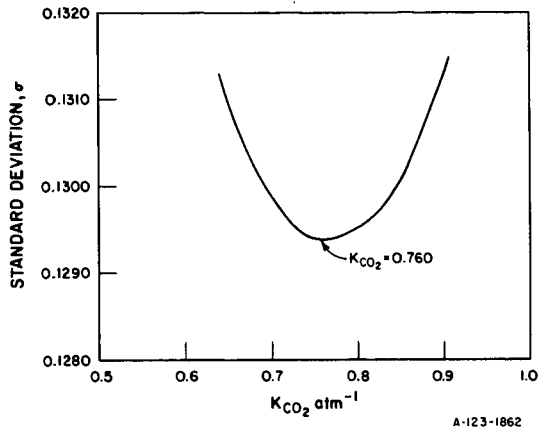
For Mechanism II, the values were slightly different, with  $A = 1.037 \times 10^{10} \text{ atm}^{-1} \text{ hr}^{-1}$ , and  $E_a = 17.90 \text{ kcal/mole}$ .

## CONCLUSION

Literature data on the rates of carbon dioxide methanation collected over a 1/2% ruthenium-on-alumina catalyst at 1 atmosphere and temperatures from 207° to 371°C have been interpreted to proceed stepwise first to carbon monoxide and ultimately to methane. Correlation of the data yielded a dependence on  $P_{\text{H}_2}$  and  $P_{\text{CO}_2}$ , both to the first power. Two possible mechanisms consistent with previous literature studies have been suggested and discussed. Rate constants, activation energies, and adsorption constants were determined.

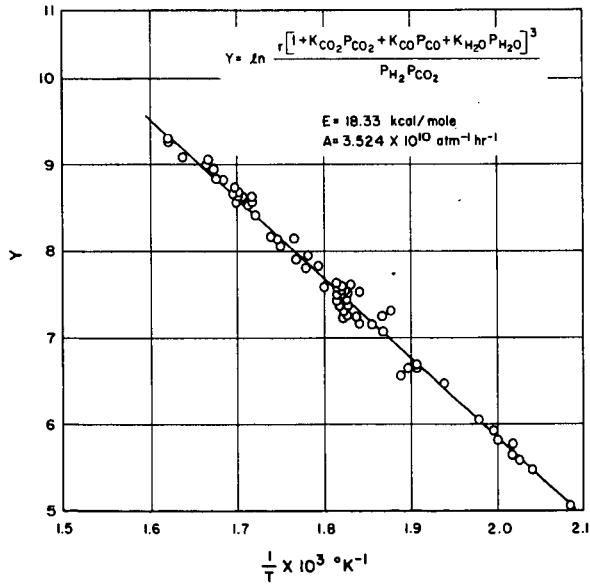
## LITERATURE CITED

1. Binder, G. G. and White, R. R., "Synthesis of Methane from Carbon Dioxide and Hydrogen," Chem. Eng. Progr. **46**, 563-574 (1950) November.
2. Bond, G. C., Catalysis by Metals. New York: Academic Press, 1962.
3. Dew, J. N., White, R. R. and Sliepcevich, C. M., "Hydrogenation of Carbon Dioxide on Nickel-Kieselguhr Catalyst," Ind. Eng. Chem. **47**, 140-146 (1955) January.
4. Doehlemann E., "The Mechanism of the Water-Gas Reaction on an Iron Catalyst," Z. Elektrochem. **44**, 178-83 (1938) [Chem. Abstr. **32**, 4060 (1938) ].
5. Emmett, P. H., Ed., Catalysis, Vol. **4**, 299-303. New York: Reinhold, 1951.
6. Gilkeson, M. M., White, R. R. and Sliepcevich, C. M., "Synthesis of Methane by Hydrogenation of Carbon Monoxide in a Tubular Reactor," Ind. Eng. Chem. **45**, 460-467 (1953) February.
7. Hougen, O. A. and Watson, K. M., "Solid Catalysts and Reaction Rates. General Principles," Ind. Eng. Chem. **35**, 529-541 (1943) May.
8. Hougen, O. A. and Watson, K. M., "Kinetics," in Chemical Process Principles. New York: John Wiley, 1947.
9. Karn, F. S., Shultz, J. F. and Anderson, R. B., "Hydrogenation of Carbon Monoxide and Carbon Dioxide on Supported Ruthenium Catalysts at Moderate Pressures," I & EC Product Res. Develop. **3**, 265-269 (1965) December.
10. Kirk, R. E. and Othmer, D. F., "Carbon Monoxide-Hydrogen Reactions," in Encyclopedia of Chemical Technology, 2nd Ed., Vol. **4**, 446-489. New York: Interscience Publishers, 1963.
11. Kul'kova, N. V. and Temkin, M. I., "Kinetics of the Reaction of Conversion of Carbon Monoxide by Water Vapor," Zh. Fiz. Khim. **23**, 695-713 (1949) [Chem. Abstr. **43**, 7308 (1949) ].
12. Kul'kova, N. V., Kuznets, Z. D. and Temkin, M. I., "The Exchange of Oxygen Isotopes Between Carbon Monoxide and Carbon Dioxide on an Iron Oxide Catalyst," Dokl. Akad. Nauk SSSR **90**, 1067-70 (1953) [Chem. Abstr. **49**, 8684 (1955) ].
13. Lunde, P. J. and Kester, F. L., "Rates of Methane Formation from Carbon Dioxide and Hydrogen Over a Ruthenium Catalyst," J. Catal. **30**, 423-429 (1973) September.
14. Oki, S. and Mezaki, R., "Identification of Rate-Controlling Steps for the Water-Gas Shift Reaction Over an Iron Oxide Catalyst," J. Phys. Chem. **77**, 447-452 (1973) February 15.
15. Oki, S. and Mezaki, R. "Mechanistic Structure of the Water-Gas Shift Reaction in the Vicinity of Chemical Equilibrium," J. Phys. Chem. **77**, 1601-1605 (1973) June 15.
16. Wagman, D. D. et al., "Heats, Free Energies, and Equilibrium Constants of Some Reactions Involving O<sub>2</sub>, H<sub>2</sub>, H<sub>2</sub>O, C, CO, CO<sub>2</sub>, and CH<sub>4</sub>." RP 1634, J. Res. Nat. Bur. Stand. **34**, 143-161 (1945).
17. Wagner, C., "Adsorbed Atomic Species as Intermediates in Heterogeneous Catalysis," in D. D. Eley, et al., Eds., Advances in Catalysis and Related Subjects, Vol. **21**, 323-81. New York: Academic Press, 1970.



A-123-1862

Figure 1. DETERMINATION OF  $CO_2$  ADSORPTION CONSTANT USING EQUATION 15, MECHANISM I



A-123-1863

Figure 2. ACTIVATION-ENERGY PLOT OF 62 DATA POINTS